DNA Trapping

DOI: 10.1002/ange.201305003

One-step Preparation of Macroporous Polymer Particles with Multiple Interconnected Chambers: A Candidate for Trapping Biomacromolecules**

*Qiuping Qian, Xiaopeng Huang, Xinyue Zhang, Zhigang Xie, and Yapei Wang**

With respect to low density and high specific surface area, porous polymer particles have been widely exploited in many applications, including ion exchange, catalytic support, purification, scavenging, microreactors, sensing, capsules for drug storage, and tissue engineering.[1] The formation of porous features relies on the availability of porogens, which traditionally involve hard templates and soft templates. The former was once popular because the pores could be created in the polymer matrix with precise control over size and shape.[2] However, the removal of hard templates requires harsh conditions, not only complicating the fabrication process, but also causing damage to the polymer matrix.[3] Soft templates consisting of various diluents are easier to remove by means of simple extraction or evaporation. Poor solvents typically engender macropores, whereas good solvents result in micropores. The encapsulation of solvents is commonly dependent on double emulsion techniques. Nonetheless, either oil-in-water-in-oil or water-in-oil-in-water processes virtually must be fulfilled through multi-step procedures.[4] To render the possibility of practical production and application, there is currently an increase in interest on research into the ease of fabrication of porous polymer particles on a large scale.[5] Simplifying the emulsion process, especially using a one-step emulsion that combines the ease of template removal and particle fabrication, is at the forefront of these efforts.

In addition to exploiting reliable methods to strengthen the ease and simplicity of fabrication, great efforts are also being devoted to manipulation of porous polymer particles for high-level applications. For example, the integration of magnetic particles enabled the synthesis of porous polymer particles that are responsive to magnetic fields.[6] Anisotropic surface functionalization improved both the water dispersion and the oil adsorption of porous polymer particles.[7] A MOF–polymer composite formed through Pickering emulsion acted as a kind of colloidosome microcapsule for effective encapsulation.[8] The capability of closing pores, by which most leaves perfectly balance their respiration and transpiration, is frequently encountered in nature. The concept of self-closing pores is a steadily developing field for porous polymer particles. The porous structures are expected to be triggered in a controlled manner, which is highly appropriate for intelligent capture or release.[9] Phase transition by thermal treatment is the major strategy to close the polymeric pores, although the closing process is slow and inconvenient.[10] Rapid self-closing by remote triggers is sought to expand the inherent functionality of porous polymer particles.

We have previously presented a versatile strategy to trigger the shape change of polymer particles by near infrared light (NIR).[11] Rapid phase transition was remotely accomplished through photothermal conversion. Herein, we reveal a one-step emulsion method to prepare macroporous polymeric microspheres with multiple interconnected chambers. Water-dispersible single-walled carbon nanotubes (SWCNTs) capable of photothermal conversion were assembled on particle surface. Taking advantage of this photothermal conversion, a rapid closing of open pores on the particle surface was directed by NIR light. The resulting porous microspheres were then used for trapping biomacromolecules such as DNA through diffusion from external solutions. DNA was eventually locked in the photoclosed polymer particles.

The synthetic route of macroporous polymeric particles was outlined in Figure 1. A typical single oil-in-water emulsion was formed between a dispersion dichloromethane phase consisting of polylactic acid (PLA) and a continuous water phase consisting of cetyltrimethyl ammonium bromide (CTAB) under vigorous agitation. Surprisingly, slow evaporation of dichloromethane from the dispersed oil droplets yielded large-dimension PLA particles with two attractive features: dimple-like surface pores and multiple interconnected chambers in the interior, as shown in Figure 1 b–d. This unique morphology is unusual, as single oil-in-water emulsion normally produces microspheres with intact surfaces. The solid particle size was critically dependent on the size of the oil droplets; relatively large particles with an average size of 18 μm were desired because such a large dimension affords great convenience for DNA capture and surface closing. Furthermore, the formation mechanism of polymer particles with unique porous features could be understood at such large dimensions (see below). Smaller porous particles could be prepared upon increasing the agitation velocity, for example,

[*] Q. Qian, X. Huang, X. Zhang, Prof. Y. Wang
Department of Chemistry, Renmin University of China
Beijing, 100872 (China)
E-mail: yapeiwang@ruc.edu.cn
Prof. Z. Xie
State Key Laboratory of Polymer Physics and Chemistry, Changchun Institute of Applied Chemistry, CAS, Changchun, 130022 (China)

[**] This work was financially supported by the Trans-Century Training Programme Foundation for the Talents by the State Education Commission (NCET-12-0530), the Fundamental Research Funds for the Central Universities, and the Research Funds of Renmin University of China (2012030065). Prof. Wenbin Du and Dongyang Cai are acknowledged for providing DNA samples.

Supporting information for this article is available on the WWW under http://dx.doi.org/10.1002/anie.201305003.

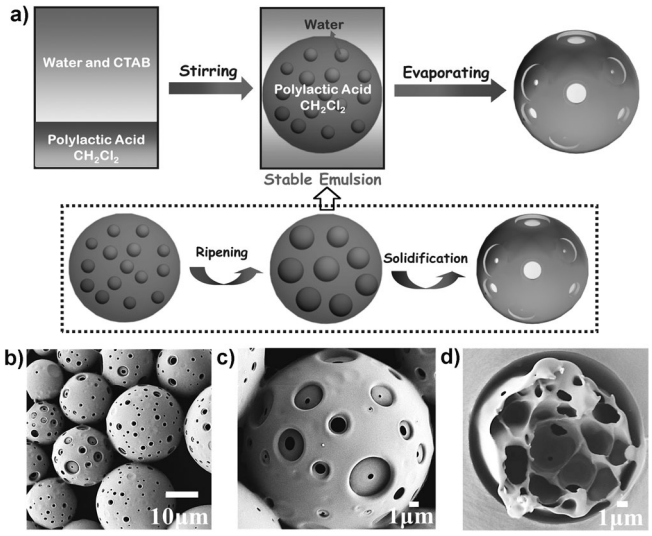

Figure 1. a) Preparation of polymer microspheres. Morphological characterizations of the polymer microspheres, SEM images of PLA microspheres (b) and (c), and interior structure of the PLA microspheres captured in an epoxy resin (d).

the average particle size dropped below 5 μm if the emulsion was produced at higher agitation velocity (10000 rpm; Supporting Information, Figure S2).

The driving force of pore formation was attributed to the conversion of emulsion droplets, from oil-in-water to water-in-oil-in-water. As shown in Figure 2c, double emulsion was apparently formed when a 10 wt% PLA dichloromethane solution was vigorously agitated in a 5% (w/v) CTAB aqueous solution. Double emulsions also appeared under other CTAB concentrations (Figure 2a,b,d). PLA is hydrophobic, and thus mainly soluble in the oil phase, as it has miltiple ester moieties, a free carboxylic acid and a free hydroxyl group at two terminals. We hypothesized that there existed a weak electrostatic interaction between PLA and CTAB that disturbed the interfacial energy. Such an interaction was assumed to lead to an influx of water from the external aqueous phase to pass through the oil/water interface, thus forming random aqueous beads in oil droplets. More water was extracted from the external aqueous phase into the oil phase upon increasing the CTAB concentration, which suggests that the porosity could be tuned by adjusting the ratio of polymer to surfactant. Gradual solvent evaporation caused a change of osmotic pressure within the oil droplet. As a result, emulsion ripening occurred in each oil droplet when the double emulsion droplets were solidified. Moreover, condensation of oil droplets led to the coalescence of internal water with the external water phase. As a consequence, surface pores and multiple interconnected chambers were generated in each polymer particle after the complete removal of solvents, as shown in Figure 2k. If the CTAB concentration dropped below 2% (w/v), the porosity in the interior of the polymer particles remained, whereas little or no surface pores were formed (Figure 2i,j). Higher CTAB concentration destroyed the unique porous morphology, creating hollow particles or bowl-like particles with entirely empty interiors. The trend of changing surface morphology with CTAB concentration increase is summarized in Figure 2m, and suggests that particle surfaces are opened wider in the presence of more CTAB. Particle morphology statistics were obtained by counting solid PLA particles in the typical SEM images. As shown in Figure 2n, 5% (w/v) is the optimized concentration for CTAB to generate macroporous particles with interconnected chambers.

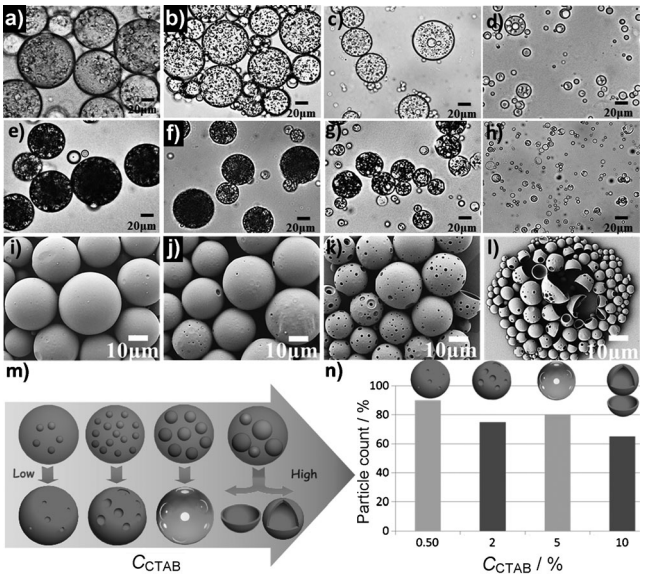

Figure 2. Optical microscopy images of oil droplets that were produced by the one-step emulsion under different CTAB concentrations: (a) 0.5% (w/v), (b) 2% (w/v), (c) 5% (w/v), (d) 10% (w/v). PLA concentration was 100 mg mL^{-1}. Microscopy images (e–h) and SEM images (i–l) of solid PLA particles that were generated from (a–d). Scale bars in (a–h) are 20 μm. m) The effect of CTAB concentration on the morphology of solid PLA particles. n) Count number of PLA particles with specific morphologies that were yielded under different CTAB concentrations.

On the basis of the above microscopic observations, a mechanism for the formation of macroporous polymer particles, using CTAB as the emulsion stabilizer, is proposed in Figure 3a. Interacting with PLA, CTAB transports water into the emulsion droplets, resulting in a phase inversion. To validate the role of polymer-surfactant interaction, other common amphiphilic additives were tested in the emulsion preparation in place of CTAB. As shown in Figure 3b,c, the emulsion droplets, generated using polyvinyl alcohol (PVA) and sodium dodecyl sulphate (SDS), respectively, did not adequately encapsulate water to produce porous polymer particles. Solid PLA particles from PVA or SDS had a compact smooth surface (Figure 3h,i). These features were retained even when the concentration of PVA or SDS was increased to 5% (w/v; Figure S4), although the particle size decreased. Whereas CTAB is a cationic surfactant, PVA is a nonionic surfactant and SDS is an anionic surfactant. As such, the interaction of PLA with PVA and SDS is relatively weak, thus impairing the formation of a double emulsion. The interaction of PLA with CTAB and SDS was straightforward when compared by FTIR (Figure S5). In the presence of CTAB, the wavenumber at 1780 cm^{-1}, which is assigned to the

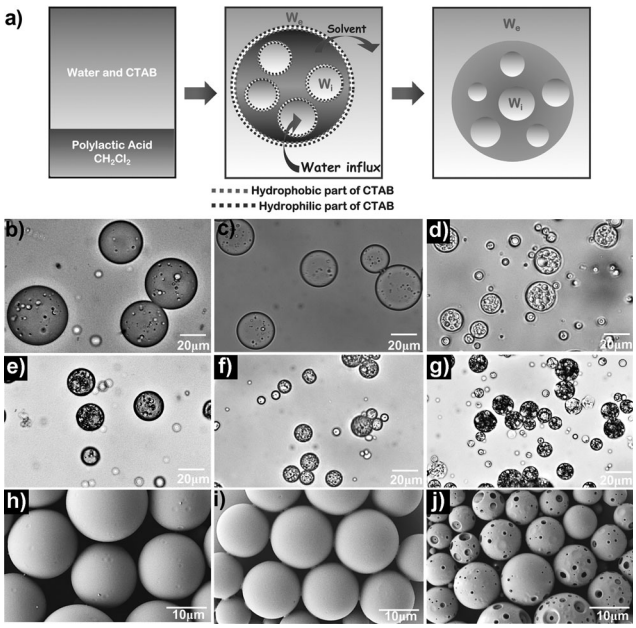

Figure 3. a) The formation of macroporous polymer particles by a one-step emulsion. Optical micrographs of PLA oil droplets after 2 min single-emulsion emulsification in the presence of b) 2% (w/v) PVA, c) 2% (w/v) SDS, and d) 5% (w/v) CTAB. Optical micrographs (e–g) and SEM images (h–j) of solid PLA particles from oil droplets (b–d) by solvent evaporation. The PLA concentration is 100 mg mL^{-1}.

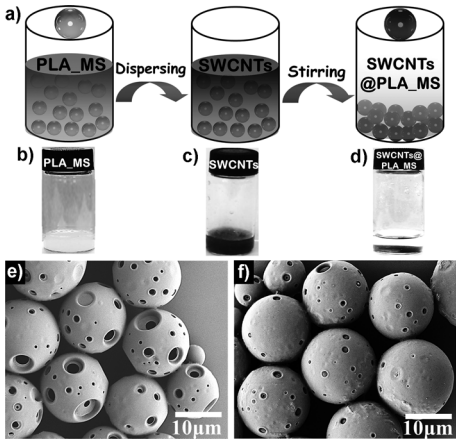

Figure 4. a) Diagram of the assembly of water-dispersible SWCNT with macroporous PLA particles. Optical images of b) a solution of well-dispersed PLA particles, c) a carboxylic-acid-functionalized SWCNT aqueous solution (0.1 mg mL^{-1}), and d) a mixture of (b) and (c) with a 1:1 volume ratio. e–f) SEM images of macroporous PLA particles without (e) and with (f) assembled SWCNTs.

stretching vibration of C=O of esters, downshifts to 1768 cm^{-1}. This shift is indicative of an interaction of the PLA polymer with CTAB. It is speculated that the quaternary ammonium salt of CTAB has a weak interaction with the ester group of PLA, although the fingerprint of the carboxylic acid was not observed. However, SDS had little effect on the stretching vibration of C=O, which indicates that the interaction between SDS and PLA is negligible. Quite a few water beads were still observed when using PVA or SDS as the surfactants. These trapped water beads ultimately induced pore formation in the interior of the solid particles, emerging as dark spots because of their distinct refractive index (Figure 3e,f). The double emulsion was due to the slightly amphiphilic feature of the natural PLA polymer. In that case, PLA polymers acted as a type of oil-soluble surfactant, stabilizing the water that was randomly plunged into the oil droplets under vigorous agitation.

Our particular interest was closing the surface pores in a controlled manner, which offers ultimately the ability to program the macroporous particles for use in targeted encapsulation. In terms of thermoplastic properties, PLA particles are generally thermal-responsive, and thus thermal annealing should be capable of triggering the self-closing of the surface pores. However, thermal treatment is not viable in most bio-applications. Local heating by photothermal conversion not only conducts the phase transition of the polymer matrix, but also minimizes damage to the surroundings. In the past, we have demonstrated that SWCNTs could transform light energy into local heat, and so direct a rapid shape change in polymer particles by NIR light.[11] Herein, water-dispersible SWCNTs functionalized with carboxylic acid groups were assembled on PLA particles to allow the remote control of a local phase transition. As shown in Figure 4d, SWCNTs immediately interacted with macroporous PLA particles that were coated with CTAB, thus indicating that a quick self-assembly occurred. The pores were fully filled in the presence of excess SWCNTs (Figure S6), although these sealed particles lost the encapsulation function. In this regard, a certain amount of SWCNTs (4.9 wt% of polymer particles, Figure S7) was recquired (Figure 4f), enough for photoresponse while still retaining porosity. The SWCNTs were mainly coated on the particle surface, and the glass transition temperature of PLA at 60 °C was not changed.

Macroporous particles assembled with SWCNTs exhibited rapid self-closing under NIR light irradiation. As shown in Figure 5b,c, the surface pores were fused and closed under NIR light for 20 min, leading to a sealed polymer particle. However, control PLA particles (without SWCNTs) had no response to NIR light (Figure S9). In principle, self-closing only occurs when the local temperature on the particle surface, or in particle interior, is above the glass-transition temperature of the PLA polymer. The mechanism of the pore-closing process has been proposed to involve multiple elements, including polymer-chain inter-diffusion driven by minimization of the energetically unfavorable interfacial area and transfer of potential energy stored in the defects.[12] Hence, we believe that the photothermal conversion of 4.9 wt% SWCNTs assembled on particles generates enough heat to trigger the local motion of surface polymers. Nonetheless, the inner pores were not closed, as the porous feature with alternating bright and dark regions was still observable by microscopy, as shown in Figure 5d. In view of the powerful penetration of NIR light, the particle interior was not assembled with SWCNTs as much as the particle surface. This issue is of vital importance, as the binding sites in the interior are still free, thus affording the possibility of effective encapsulation.

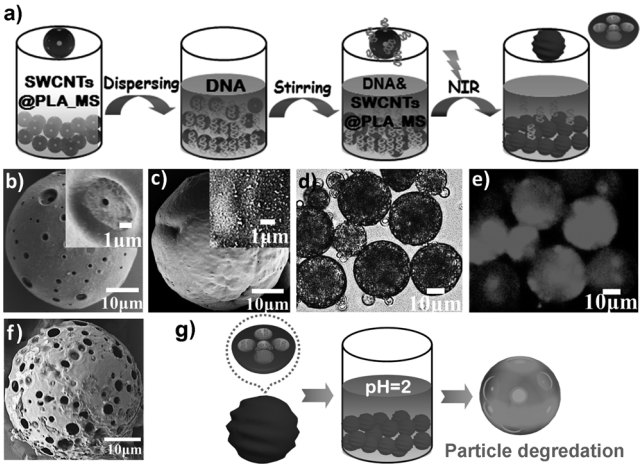

Figure 5. a) The process of DNA trapping in the PLA particles. SEM images of b) SWCNTs-coated PLA particles before self-closing, and c) after self-closing by NIR light (808 nm, 8 $W cm^{-2}$). The bright-field (d) and fluorescent (e) images of PLA microcapsules loaded with a number of DNA molecules. f) An SEM image of pore-reopened PLA particles. g) Pore reopening upon degradation of PLA; the self-closed particles were suspended in an aqueous solution at pH 2 for 5 days.

Taking advantage of self-closing porous particles for trapping excess biomacromolecules such as DNA and RNA may be a new way to treat uncontrolled inflammation. Redundant extracellular nucleic acids from a large area of dead and dying cells is a promoter of uncontrolled inflammation, which happens frequently to patients with severe burns or injuries.[13] Self-closing porous particles are good candidates because they can both catch and hold the biomacromolecules. With this purpose in mind, we investigated whether DNA molecules could be trapped and sealed in the macroporous PLA particles. A typical DNA trapping process is illustrated in Figure 5a. First, a powder of solid porous PLA microspheres (200 mg) coated with SWCNTs was dispersed in a diluted fluorescein-labeled DNA solution (0.01 $mg mL^{-1}$ in PBS buffer). Second, after adequate adsorption under a gentle stirring, over 85% DNA molecules were loaded into the porous PLA particles (Figure S11). Third, the surface pores of PLA particles were closed by NIR light, permanently encapsulating DNA molecules in the particles. Figures 5b and 5c summarize the surface morphologies of the PLA microspheres before and after NIR light irradiation. As already noted, only the surface pores were closed by NIR light, thus the surface of inner pores retained positively charged because of the CTAB. DNA molecules with negative charges were successfully loaded and sealed in the PLA particles, as shown in Figure 5e. We believe that this method offers promise for hampering the effect of excess nucleic acids on immune system. In terms of biodegradable performance, the closed PLA particles are envisioned to be degraded in the biological environmental condition for a sufficiently long time, leading to a slow reopening of surface pores. Harsh conditions using a low pH buffer could accelerate the degradation of PLA polymer to quickly reopen the closed particles. As shown in Figure 5f,g, surface pores appeared if the photo-closed PLA particles were kept in a buffer solution at pH 2.0 for 5 days. It should be noted that, for potential clinical applications, these harsh conditions are not necessary anymore. Prolonging the containment of nucleic acids is helpful for tailoring the elimination of uncontrolled nucleic-acid-sensing inflammatory diseases.

In conclusion, we have demonstrated a straightforward and generally applicable one-step method to fabricate macroporous polymer particles with multiple interconnected chambers. To the best of our knowledge, this is the first example of the preparation of such porous particles in such a simple (one-step), inexpensive (no complicated facilities required) and large-scale (merely dependent upon the amount of raw materials) way, that is promising for practical production and application. Polymer particles assembled with SWCNTs were shown to be able to close their surface pores under NIR light, acting as a kind of smart container to encapsulate and hold free DNA molecules by remote control. The encapsulation of nucleic acids is of vital importance for curing uncontrolled inflammation. It is believed that this line of research can be extended to the controllable encapsulation of other biomacromolecules, for example, biomarkers that are created from tumor cells. More interestingly, a reversible reopening of the surface pores was accomplished by partial degradation of the polymer particles, thus affording the possibility for controlled release after a controlled encapsulation. Some disadvantages still remain to be surmounted, particularly particle uniformity, distribution of pore size, and the speed of light response. Solving these problems could allow for this system to be taliored for real bio-application, as well as catalysis, separation, sensors, and healthcare.

Received: June 11, 2013
Revised: July 2, 2013
Published online: August 12, 2013

Keywords: DNA trapping · near infrared light · photothermal conversion · polymers · synthetic methods

[1] a) D. C. Sherrington, *J. Polym. Sci. Part A* **2001**, *39*, 2364–2377; b) J. Lu, P. H. Toy, *Chem. Rev.* **2009**, *109*, 815–838; c) C. Lin, W. Zhu, H. W. Yang, Q. An, C. A. Tao, W. N. Li, J. C. Cui, Z. L. Li, G. T. Li, *Angew. Chem.* **2011**, *123*, 5049–5053; *Angew. Chem. Int. Ed.* **2011**, *50*, 4947–4951; d) P. H. Seeberger, *Nature* **2009**, *1*, 258–260; e) Y. J. Jiang, Q. Y. Sun, L. Zhang, Z. G. Jiang, *J. Mater. Chem.* **2009**, *19*, 9068–9074; f) J. B. Fan, C. Huang, L. Jiang, S. T. Wang, *J. Mater. Chem. B* **2013**, *1*, 2222–2235.

[2] a) C. T. Kresge, M. E. Leonowicz, W. J. Roth, J. C. Vartuli, J. S. Beck, *Nature* **1992**, *359*, 710–712; b) A. Tuncel, M. Tuncel, B. Salih, *J. Appl. Polym. Sci.* **1999**, *71*, 2271–2290; c) J. W. Kim, J. H. Ryu, K. D. Suh, *Colloid Polym. Sci.* **2001**, *279*, 146–152; d) G. H. Ma, H. Sone, S. Omi, *Macromolecules* **2004**, *37*, 2954–2964; e) X. Dong, X. Wu, H. Rong, M. Zhen, Z. Cheng, *Chem. Mater.* **2005**, *17*, 5891–5892; f) J. B. Nama, J. H. Ryua, J. W. Kimb, I. S. Changb, K. D. Suh, *Polymer* **2005**, *46*, 8956–8963; g) X. D. He, X. W. Ge, H. R. Liu, M. Z. Wang, Z. C. Zhang, *J. Polym. Sci. Part A* **2007**, *45*, 933–941; h) J. Li, Y. H. Wang, C. L. Zhang, F. X. Liang, X. Z. Qu, J. L. Li, Q. Wang, D. Qiu, Z. Z. Yang, *Polymer* **2012**, *53*, 3712–3718.

[3] a) G. Wang, P. F. Zhang, H. J. Dou, W. W. Li, K. Sun, X. T. He, J. S. Han, H. S. Xia, Y. Li, *Langmuir* **2012**, *28*, 6141–6150;

b) A. K. Nyhus, S. Hagen, A. Berge, *J. Appl. Polym. Sci.* **2000**, *76*, 152 – 169.

[4] a) P. B. O'Donnell, J. W. McGinity, *Adv. Drug Delivery Rev.* **1997**, *28*, 25 – 42; b) W. Q. Zhou, T. Y. Gu, Z. G. Su, G. H. Ma, *Eur. Polym. J.* **2007**, *43*, 4493 – 4502; c) J. A. Hanson, C. B. Chang, S. M. Graves, Z. Li, T. G. Mason, T. J. Deming, *Nature* **2008**, *455*, 85 – 88; d) H. Y. Chen, Y. Zhao, Y. L. Song, L. Jiang, *J. Am. Chem. Soc.* **2008**, *130*, 7800 – 7801; e) F. Gao, Z. G. Su, P. Wang, G. H. Ma, *Langmuir* **2009**, *25*, 3832 – 3838; f) S. W. Choi, Y. Zhang, Y. Xia, *Adv. Funct. Mater.* **2009**, *19*, 2943 – 2949; g) J. Lee, Y. J. Oh, S. K. Lee, K. Y. Lee, *J. Controlled Release* **2010**, *146*, 61 – 67; h) C. J. Ke, T. Y. Su, H. L. Chen, H. L. Liu, W. L. Chiang, P. C. Chu, Y. Y. Xia, H. W. Sung, *Angew. Chem.* **2011**, *123*, 8236 – 8239; *Angew. Chem. Int. Ed.* **2011**, *50*, 8086 – 8089; i) J. X. Xu, G. J. Chen, R. Yan, D. Wang, M. C. Zhang, W. Q. Zhang, *P. C. Sun, Macromolecules* **2011**, *44*, 3730 – 3738.

[5] a) H. F. Zhang, D. Edgar, P. Murray, A. Rak-Raszewska, L. Glennon-Alty, A. I. Cooper, *Adv. Funct. Mater.* **2008**, *18*, 1 – 7; b) I. Kim, H. J. Byeon, T. H. Kim, E. S. Lee, K. T. Oh, B. S. Shin, K. C. Lee, Y. S. Youn, *Biomaterials* **2012**, *33*, 5574 – 5583; c) X. M. Na, F. Gao, L. Y. Zhang, Z. G. Su, G. H. Ma, *ACS Macro Lett.* **2012**, *1*, 697 – 700.

[6] L. L. Zhao, L. J. Zhu, Q. Wang, J. L. Li, C. L. Zhang, J. G. Liu, X. Z. Qu, G. L. He, Y. F. Lu, Z. Z. Yang, *Soft Matter* **2011**, *7*, 6144 – 6150.

[7] A. Abbaspourrad, N. J. Carroll, S. H. Kim, D. A. Weitz, *Adv. Mater.* **2013**, *25*, 3215 – 3221.

[8] J. Huo, M. Marcello, A. Garai, D. Bradshaw, *Adv. Mater.* **2013**, *25*, 2717 – 2722.

[9] S. E. Reinhold, K. G. Desai, L. Zhang, K. F. Olsen, S. P. Schwendeman, *Angew. Chem.* **2012**, *124*, 10958 – 10961; *Angew. Chem. Int. Ed.* **2012**, *51*, 10800 – 10803.

[10] S. H. Im, U. Jeong, Y. N. Xia, *Nat. Mater.* **2005**, *4*, 671 – 675.

[11] X. P. Huang, Q. P. Qian, X. Y. Zhang, W. B. Du, H. P. Xu, Y. P. Wang, *Part. Part. Syst. Charact.* **2013**, *30*, 235 – 240.

[12] R. P. Wool, *Soft Matter* **2008**, *4*, 400 – 418.

[13] J. Lee, J. W. Sohn, Y. Zhang, K. W. Leong, D. Pisetsky, B. Sullenger, *Proc. Natl. Acad. Sci. USA* **2011**, *108*, 14055 – 14060.

